ELSEVIER

Quaternary Science Reviews 27 (2008) 769–780

QSR

Cold and wet Last Glacial Maximum on Mount Sandıras, SW Turkey, inferred from cosmogenic dating and glacier modeling

Mehmet Akif Sarıkaya[a,*], Marek Zreda[a], Attila Çiner[b], Chris Zweck[a]

[a]*Hydrology and Water Resources Department, University of Arizona, Tucson, AZ 85721, USA*
[b]*Geological Engineering Department, Hacettepe University, Beytepe, Ankara 06800, Turkey*

Received 3 July 2007; received in revised form 18 December 2007; accepted 3 January 2008

Abstract

In situ cosmogenic ^{36}Cl was measured in boulders from moraines on Mount Sandıras (37.1°N, 28.8°E, 2295 m), the southwestern most previously glaciated mountain in Turkey. Valleys on the north side of the mountain were filled with 1.5 km long glaciers that terminated at an altitude of 1900 m. The glacial activity on Mount Sandıras correlates with the broadly defined Last Glacial Maximum (LGM). The maximum glaciation occurred approximately 20.4 ± 1.3 ka (1σ; 1 ka = 1000 calendar years) ago, when glaciers started retreating and the most extensive moraines were deposited. The glaciers readvanced and retreated by 19.6 ± 1.6 ka ago, and then again by 16.2 ± 0.5 ka. Using the glacier modeling and the paleoclimate proxies from the Eastern Mediterranean, we estimated that if temperatures during LGM were 8.5–11.5 °C lower than modern, precipitation was up to 1.9 times more than that of today. Thus, the local LGM climate was cold and wet which is at odds with the conventional view of the LGM as being cold and dry in the region.

1. Introduction

The evidence of past glacial activities in mountain settings provides direct information of the magnitude and frequency of past climate changes. Because of the unique location of Turkey in the transition zone between the temperate Mediterranean climates influenced by North Atlantic cyclones (Macklin et al., 2002) and the subtropical high pressure climatic zone (la Fontaine et al., 1990), the paleoclimate of Turkey is highly sensitive to climatic perturbations that affect the position and/or intensity of the westerly storm tracks that carry moisture from the North Atlantic and Mediterranean Sea. Thus, studying the timing and extent of past glacial activity as a proxy of past climates on Turkey can reveal valuable information on Late Quaternary climate changes.

Several mountain ranges in Turkey supported glaciers during the Late Quaternary (Erinç, 1952; Messerli, 1967; Birman, 1968; Kurter and Sungur, 1980; Çiner, 2004; Akçar et al., 2007). Among these, the Taurus Mountain Range, in south Anatolia, has two-thirds of the previously glaciated mountains in the country. On the far east (Fig. 1), Mount Cilo (4135 m) has the largest glaciated area in Turkey, including ice caps and valley glaciers up to 4 km long (Kurter, 1991). In the central Taurus, Mount Aladağlar (3756 m) has a well-preserved moraine record of extensive Early Holocene glaciers (Klimchouk et al., 2006; Zreda et al., 2006). While much lower than their eastern counterparts, the western Taurides also have several mountains with evidence of Pleistocene glaciers. Mount Dedegöl (2990 m, Zahno et al., 2007), Beydağ (3086 m, Messerli, 1967), Akdağ (3016 m, Onde, 1952) and Sandıras (2295 m, de Planhol, 1953; Doğu, 1993) (Fig. 1) show several cirques and well-preserved glacier related landforms especially on their north and northeast facing slopes. Today, due to the increasing effect of continentality from west to east in Anatolia, western mountains experience wetter and warmer climate than the eastern mountains. Today, active glaciers are present only in central and eastern mountains, and their sizes are increasing from west to east. Additionally, Late Pleistocene equilibrium line altitude (ELA) estimates in Turkey support this continental effect (Messerli, 1967; Erinç,

*Corresponding author. Tel.: +1 520 621 4072; fax: +1 520 621 1422.
E-mail address: sarikaya@email.arizona.edu (M.A. Sarıkaya).

0277-3791/$ - see front matter © 2008 Elsevier Ltd. All rights reserved.
doi:10.1016/j.quascirev.2008.01.002

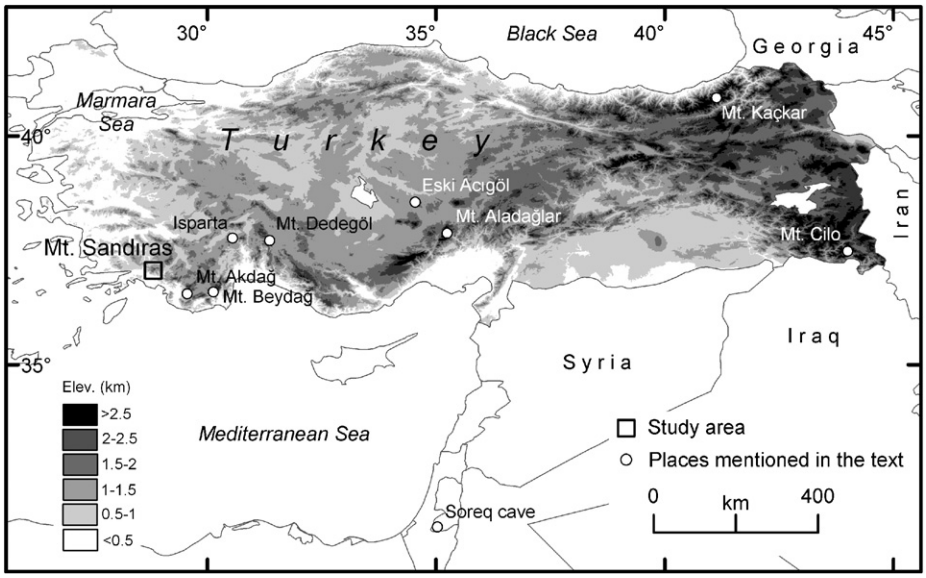

Fig. 1. Digital elevation model of Turkey and locations of places discussed in the text.

1971, 1978; Atalay, 1987). During the Last Glacial Maximum (LGM, 21,000 calendar years ago), western Anatolian mountains had ELAs as low as 2000–2400 m while eastern mountains had ELAs about 3000–3200 m.

Glacial deposits in all these mountains have been studied to some degree, but few of them have been dated numerically. Most of the age estimates for glacial deposits are based on relative dating techniques, including stratigraphic relationships, degree of weathering and soil development (de Planhol, 1953; Birman, 1968; Doğu, 1993). Generally, previous studies assigned Late Pleistocene to the age of glaciation in the southwest Taurus Mountains (de Planhol, 1953; Doğu, 1993; Çiner, 2004 and references therein).

The glacial landforms on Mount Sandıras were mapped and their lithostratigraphy described in detail by de Planhol (1953) and Doğu (1993). However, because these glacial deposits have not been dated numerically, the exact timing of glaciations is unknown, which precludes paleoclimatic interpretation based on the glacial records. In this study, we examined the timing (from the age of landforms) and magnitude (from the position of ice margins) of paleoclimatic changes on Mount Sandıras by using the cosmogenic ^{36}Cl exposure dating method. We modeled the glacier response to climatic changes using a glacier model to reconstruct temperature and precipitation at the time of glaciation. Finally, we compared our paleoclimatic findings with other Late Quaternary climate proxies from the Eastern Mediterranean region.

2. Physical setting and climate

Mount Sandıras (37.1°N, 28.8°E, 2295 m above mean sea level), also known as Çiçekbaba (Flower father, in Turkish), Sandras or Gölgeli Dağları (Shaded Mountains), is the southwestern most previously glaciated mountain in the Anatolian Peninsula (Fig. 1). The mountain is located about 40 km from the Mediterranean coast. The land elevation increases rapidly towards inland creating a natural climatic barrier between the coastal area and the interior.

The summit of Mount Sandıras is a plateau approximately 1 km^2 in area, sloping to the southeast and ranging in elevation from 2200 to 2295 m (Fig. 2). The geological formation exposed on the mountain is the upper part of the Lycian Allochthons, called Lycian Peridotite Thrust Sheet (Collins and Robertson, 1998). It consists predominantly of serpentinized harzburgite, with minor pyroxenite, pediform dunite and chromitite (Kaaden, 1959; de Graciansky, 1967; Engin and Hirst, 1970; Collins, 1997).

Present climate in southwest Turkey is characterized by dry/hot summers and wet/temperate winters (Kendrew, 1961). Average summer temperature (June, July and August; JJA) on the southwest Mediterranean coast of Turkey is about 26 °C (calculated from long-term weather stations data downloaded from Global Historical Climatology Network, version 2, http://www.ncdc.noaa.gov/oa/climate/ghcn-monthly/index.php, accessed in May 2007), and average winter temperature (December, January and February; DJF) is about 10 °C. Winters are moderately wet. Sixty percent of average 0.9 m annual precipitation falls in winter months (DJF) due to the penetration of depressions that brings moisture from either the Atlantic Ocean or the Mediterranean Sea (Stevens et al., 2001). These storm tracks tend to move eastward along the Mediterranean (Kendrew, 1961; Wigley and Farmer, 1982) and bring most of the precipitation in the winter. Summers are dry. Only 2% of annual precipitation falls in summer months (JJA) due to the persistent northerly winds (Kendrew, 1961).

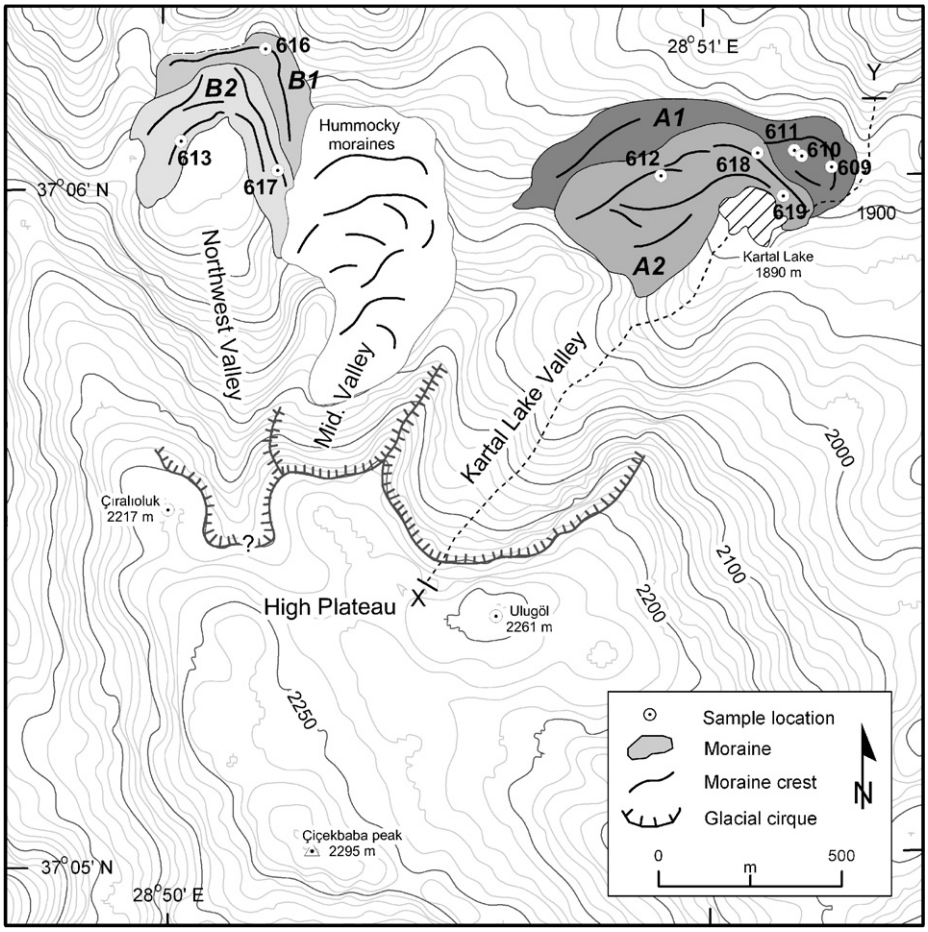

Fig. 2. Glacial features of Mount Sandıras with sample locations and the central ice flow line (dashed line between *X* and *Y*) along which the glacier was modeled.

3. Evidence of glacial action on Mount Sandıras

Philippson (1915), cited by Doğu (1993), first described evidence of former glaciations on Mount Sandıras. de Planhol (1953) suggested that an ice cap covered the flat top of the mountain during the Würm glacial age and the tongues of that ice cap reached an altitude of 1900 m on the north side. He calculated the Würm glaciation snow line (similar to ELA) to be at 2000–2050 m and proposed that this snow line lower than that on other mountains in southwestern Turkey is due to the tectonic lowering of Sandıras that occurred after the glaciation. However, the position of river terraces on the southern slopes of the mountain suggests at least 20–30 m of uplift (Pons and Edelman, 1963; Doğu, 1986, 1994), invalidating the idea of de Planhol (1953).

Messerli (1967) rejected the tectonic hypothesis of de Planhol (1953), and proposed that the low ELA was due to the local climatic conditions that occurred during the Würm glacial age and due to the proximity of Mount Sandıras to the source of moisture in the adjacent sea. He described glacial evidence from nearby Akdağ and Beydağ (Fig. 1), and calculated the local Würm snow line on these mountains to be 2500–2600 m.

Doğu (1993) mapped and described glacial deposits from the summit plateau and from the valleys on the northern and northeastern flanks of the mountain. He found that the northern valleys were glaciated during two epochs of the Würm glaciation. During the first epoch, the plateau was covered by an ice cap whose outlet glaciers reached lower elevations via northern valleys. During the second epoch, the ice cap did not exist and only small valley glaciers existed in the northern valleys. According to de Planhol (1953) and Doğu (1993), the high plateau above 2200 m (Fig. 2) is a remnant of an old erosional level (peneplane) which was modified by an ice cap during the Late Pleistocene. But our own field work revealed no clear evidence of glacial action on the plateau. It is likely that the combination of southern exposure, flat topography and strong winds prevented accumulation of snow and ice even during glacial times.

The northern valleys (the Kartal Lake Valley, the Middle Valley and the Northwest Valley, Fig. 2) contain the most important glacial features on the Mount Sandıras. Kartal Lake Valley, a typical U-shaped glacial valley, 400–550 m wide, extends 1.5 km down from the plateau at an altitude of 2220 m to the lowest moraine below Kartal Lake at about 1900 m (Fig. 2). The highest part of the valley is

occupied by a large glacial cirque with nearly vertical walls that are 100 m high. Doğu (1993) interpreted this sharp edge as evidence of a two-stage glaciation, but this type of sharp morphology is a characteristic of cirques (Ehlers, 1996) and is not a proof of multiple glaciations. The Kartal Lake Valley continues with two consecutive steps at around 2090 and 2000 m. In the lower part of the valley, there are several terminal and lateral moraines between 1900 and 2000 m. The moraines of Kartal Lake Valley have many crests (marked in Fig. 2) separated by depressions several meters deep, indicating small fluctuations of the ice margin. The stratigraphic positions of the moraine crests and age results (Section 5.1) suggest that at least two separate sets of moraine exist in the Kartal Lake valley. The older moraines (A1) are the farthest crests below the lake, and the younger ones (A2) are the moraines closest to the lake (Fig. 2). Several left lateral moraine crests also exist on the northwest of the lake, in continuation with the terminal moraines A1 and A2. On the right side of the valley, there are no remnants of glacial deposits other than small patches of till on the bedrock.

The Northwest Valley (Fig. 2) starts east of Çıralıoluk Tepe (2217 m) and continues north–northwest from about 2210 m to 1900 m. The cirque area is not as well developed as that in the Kartal Lake Valley, but can be outlined by steep bedrock walls. The valley has two well-preserved loops of terminal and lateral moraines, B1 and B2, at elevations of about 1900 and 1930 m, respectively. These moraines are dissected by melt water and small streams. The outer part of the lower terminal moraine (B1) has a very fresh surface and steep slope (~60°) on the down valley side, indicating that the outer part of B1 was removed recently. On the topographic maps from 1950s, the outer part of the crest still existed, but our GPS surveys and field observations indicate that this part is missing. This shows that at least part of the moraine is missing, and suggests that if older moraines ever existed in the valleys, they might have been obliterated.

The Middle Valley (Fig. 2) has numerous crescent-like nested crests separated from each other by small depressions. These hummocky moraines of the Middle Valley start at an elevation of about 2100 m and continue to about 1950 m. Boulders here are generally small and not well preserved. Because of the lack of suitable boulder to date by cosmogenic methods, we did not collect any sample from this valley.

4. Methods

4.1. Cosmogenic ^{36}Cl dating of moraines

4.1.1. Determination of ^{36}Cl ages

We used the cosmogenic ^{36}Cl method (Davis and Schaeffer, 1955; Phillips et al., 1986; Zreda and Phillips, 2000) to determine surface exposure ages of boulders from moraines associated with the Sandıras glaciation. Chlorine 36 is produced in rocks by collisions of cosmic-ray neutrons and muons with atoms of Cl, Ca and K (Zreda et al., 1991). Once produced, it remains in place and accumulates continuously with time (Zreda and Phillips, 2000). Because the production rates of ^{36}Cl from the three target elements are known, at least in principle (Zreda et al., 1991; Phillips et al., 1996, 2001; Stone et al., 1996, 1998; Swanson and Caffee, 2001; Zweck et al., 2006), measured concentrations of ^{36}Cl in rocks can be used to determine how long these rocks have been exposed to cosmic radiation. In situ accumulation of various cosmogenic nuclides, including ^{36}Cl, has been used to develop glacial chronologies in many areas (Zreda et al., 1999; Owen et al., 2001, 2002; Mackintosh et al., 2006; Principato et al., 2006; Akçar et al., 2007) and the approach is considered reliable.

The inventory of cosmogenic nuclide in the dated material depends on the geographic location of the sample (latitude, longitude and elevation) as well as amount of shielding of the sample by surrounding topography and snow from exposure to cosmic rays, the concentration of the target elements and assumed elemental production rates. The location dependence of ^{36}Cl production was calculated using Desilets and Zreda (2003) and Desilets et al. (2006a). Topographic shielding corrections were made by measuring the inclination to the horizon of the sample locations at 45° azimuthal increments using a hand-held clinometer and applying the method given in Gosse and Phillips (2001, pp. 1520–1522). Snow corrections were made by estimating the average annual snow thickness on sample sites using the long-term precipitation and temperature data from nearby weather stations and interpolating them to Mount Sandıras by the method described in Section 4.2. The shielding correction factors are given in Table 1.

Cosmogenic ^{36}Cl surface exposure ages were calculated using a new approach that is being implemented in the ACE (Age Calculation Engine) software (Anderson et al., 2007), previously known as iCronus (Zweck et al., 2006), using the following production rates: 71.7 ± 3.2 atoms ^{36}Cl $(\mathrm{g\,Ca})^{-1}\,\mathrm{yr}^{-1}$, 155 ± 8.0 atoms ^{36}Cl $(\mathrm{g\,K})^{-1}\,\mathrm{yr}^{-1}$ and 678 ± 43 fast neutrons $(\mathrm{g\,air})^{-1}\,\mathrm{yr}^{-1}$. These rates are based on the calibration data set of Phillips et al. (1996). They have been scaled to sea level (atmospheric pressure $1033\,\mathrm{g\,cm}^{-2}$) and high geomagnetic latitude (geomagnetic cutoff rigidity <2 GV) using Desilets and Zreda (2003) and Desilets et al. (2006a), and include necessary corrections for secular changes in paleomagnetic intensity (Guyodo and Valet, 1999; Yang et al., 2000), changes in geomagnetic pole position (Ohno and Hamano, 1992) and eustatic changes in seal level (Fairbanks, 1989). As an example, time variation of cosmogenic ^{36}Cl production rate for sample SA02-609 is given in Fig. 3 along with its time averaged rate. Other ^{36}Cl production rate estimates are also available (Stone et al., 1996, 1998; Swanson and Caffee, 2001), which would result in different age estimates for the samples. However, we prefer to use the production rates based on the data set of Phillips et al. (1996) because (a) in this data set, ^{36}Cl production rates have been

Table 1
Locations, shielding correction factors, sample thicknesses, measured total ^{36}Cl inventories, time averaged total production rates and ^{36}Cl ages of boulders with moraine ages of Sandıras glaciations

Sample	Moraine	Elev. (m)	Lat. (°N)	Long. (°E)	Shielding correction[b]	Sample thickness (cm)	$^{36}Cl_{Total}$ (10^4 atoms g^{-1})	Production rate[c] (atoms g^{-1} yr^{-1})	Boulder age[d] (ka)	Moraine age[e] (ka)
Kartal Lake Valley										
SA02-609	A1	1899	37.100	29.854	0.9898	4	30.6±4.6	14.2	22.1±3.3	20.4±1.3 (±1.6)
SA02-610	A1	1902	37.100	28.853	0.9698	2	28.8±1.5	15.0	19.6±1.0	
SA02-611	A1	1902	37.100	28.853	0.9898	3	39.1±4.0	19.5	20.6±2.1	
SA02-612	A2	1949	37.100	28.849	0.9898	2	67.9±11.5	40.4	17.2±2.9	19.6±1.6 (±1.8)
SA05-618	A2	1914	37.100	28.852	0.9798	3	34.5±1.4	17.9	19.2±0.8	
SA05-618-A	A2	1914	37.100	28.852	0.9789	3	35.0±1.4	16.1	21.9±0.9	
SA05-619[a]	A2	1910	37.099	28.852	0.9895	1.5	63.0±2.3	18.9	34.7±1.3	
Northwest Valley										
SA05-616	B1	1907	37.103	28.837	0.9886	1	21.4±1.8	14.7	14.8±1.2	16.5±1.1 (±1.3)
SA05-616-A	B1	1907	37.103	28.837	0.9886	1	26.2±0.9	15.5	17.2±0.6	
SA05-613[a]	B2	1934	37.101	28.834	0.9627	2	6.3±0.4	12.4	5.1±0.3	16.2±0.5 (±0.8)
SA05-617	B2	1934	37.100	28.837	0.9789	3	34.1±1.6	21.2	16.4±0.8	
SA05-617-A	B2	1934	37.100	28.837	0.9789	3	37.2±1.6	23.7	16.0±0.7	

[a]Samples that are not included in the moraine age calculations.
[b]The product of topographic and snow correction factors.
[c]Time averaged total production rate of ^{36}Cl at the surface of the boulder.
[d]Uncertainties are based on analytical errors and given in $1\sigma_d$ (standard deviation) level. Replicates were integrally averaged before adding to the moraine age calculations.
[e]Uncertainties are based on boulder-to-boulder variability and given in $1\sigma_{em}$ (standard error of the mean) level. Total errors which also include uncertainties on production rates of ^{36}Cl are given in parentheses.

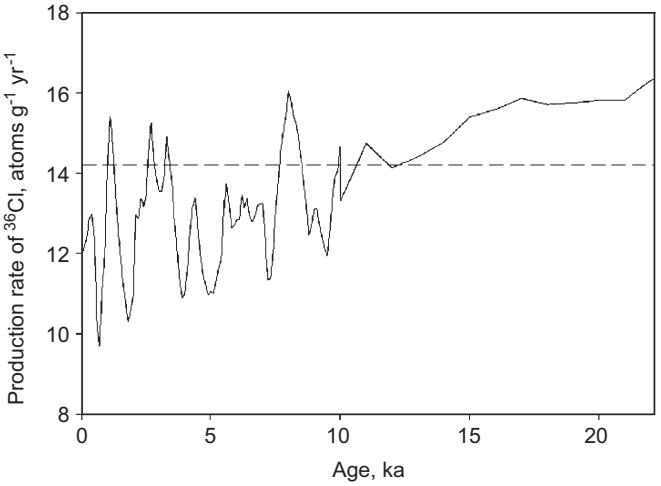

Fig. 3. Cosmogenic ^{36}Cl production rate variation of sample SA02-609 for 22.1 ka. The variations about the mean of 14.2 (horizontal line) are due to the combination of changes in the geomagnetic intensity and sea level (gradually decreasing long term change) and magnetic pole position (short term fluctuations).

determined using many samples of different ages and from different localities while other production rates are based on fewer samples and/or fewer localities; (b) ^{36}Cl production rates from all three primary target (Ca, K and Cl) have been calculated simultaneously and (c) computational procedures used for the calibration samples and for our samples in this research were identical, which assures compatibility of all results.

4.1.2. Collection, preparation and analysis of samples

We collected samples for cosmogenic ^{36}Cl dating from the top few centimeters of boulders using a hammer and chisel. Boulders were chosen based on their preservation, size, appearance and position on the landform. We sampled the boulders on the crests of the moraines and restricted sampling to large (usually $\geqslant$1 m in diameter) boulders that have a strong root in the moraine matrix. The aim of this sampling strategy was to minimize potential effects of post-depositional complications, such as boulder rolling or matrix erosion and gradual exposure of boulders. We also avoided sampling surfaces with evidence of spalling, weathering and other visible signs of surface modification. In the field, we measured the thickness of each sample (given in Table 1) to calculate the depth-integrated production rates.

Samples were crushed and sieved to separate the 0.25–1.0 mm size fraction, which was leached with 5% HNO_3 overnight and rinsed in deionized water to remove atmospheric ^{36}Cl. Chlorine was liberated from silicate matrix using high pressure acid digestion bombs (Almasi, 2001; Desilets et al., 2006b), precipitated as AgCl, purified of sulfur (^{36}S is an isobar of ^{36}Cl and interferes with the measurement of ^{36}Cl), and the ^{36}Cl/Cl was measured with accelerator mass spectrometry (AMS) at PRIME Lab, Purdue University, Indiana, USA. Samples SA05-618-A, 616-A and 617-A (Table 1) which are replicates of SA05-618, 616 and 617, respectively, were prepared in open vessels (Desilets et al., 2006b) to compare with samples prepared in high pressure acid digestion bombs. Total Cl was estimated using the ion specific electrode method (Aruscavage and Campbell, 1983; Elsheimer, 1987) at the University of Arizona, and its precise determination was made from measurement of ^{37}Cl/^{35}Cl on spiked samples (Desilets et al., 2006b) after the AMS measurement of ^{36}Cl/Cl.

Major and trace elements that have high thermal neutron cross-sections (B, Sm, Gd and others) compete with ^{35}Cl for thermal neutrons and must be taken into account when calculating cosmogenic production rates. Major elements were measured with inductively coupled plasma atomic emission spectroscopy (ICP-AE), selected trace elements were measured with inductively coupled plasma mass spectrometry (ICP-MS), and boron was measured with prompt gamma-neutron activation analysis (PGNAA), all at Activation Laboratories Inc., Ont., Canada (Table 2).

4.2. Glacier modeling

To investigate the response of Mount Sandıras glaciers to climate change, we used a one-dimensional ice flow model (Paterson, 1994; Haeberli, 1996) to simulate changes in ice extent. The model allows the user to recreate a valley glacier along an ice flow line as a function of prescribed surface air temperature and precipitation. Starting from the present day valley topography and time invariant mass balance patterns, the model builds up a glacier until a steady-state condition (equilibrium) is reached.

The model calculates the ice mass balance using the accumulation of ice predicted by snowfall modeled as precipitation occurring below zero degrees and ablation of ice by using positive degree day factors, which assume a correlation between the sum of positive air temperatures and the amount of ablation of ice (Braithwaite, 1995). Our model assumes no basal sliding and the ice is assumed to be isothermal. Initially, we applied the glacier model to both the Kartal Lake Valley and the Northwest Valley. The results showed no significant difference in the response to climatic signal, which means that the valleys have similar responses to climate change. We limited further modeling to the Kartal Lake Valley because the most extensive and best preserved moraines are in this valley, the source area (cirque) is well developed, and our cosmogenic ages show at least two glacial advances (Section 5.1).

The required inputs for the glacier model are: (1) the surface topography; (2) the spatial distribution of the modern day monthly mean temperatures and (3) the precipitation rates along the glaciated valley. Surface topography was constructed from 1/25,000 scale topographic map along the

Table 2
Analytical results of samples from Mount Sandıras

Element	Na_2O	MgO	Al_2O_3	SiO_2	P_2O_5	K_2O	CaO	TiO_2	MnO	Fe_2O_3	LOI[a]	Total	B	Sm	Gd	U	Th	Cl	$^{36}Cl/(10^{15}$ Cl)
Units	%	%	%	%	%	%	%	%	%	%	%	%	ppm	ppm	ppm	ppm	ppm	ppm	
Detection limit	0.01	0.01	0.01	0.01	0.01	0.01	0.01	0.001	0.001	0.01	0.01		0.5	0.1	0.1	0.1	0.1		
Kartal Lake Valley																			
SA02-609	0.23	39.05	2.20	45.02	0.02	0.09	2.12	0.029	0.116	8.34	2.66	99.9	<0.5	<0.1	<0.1	<0.1	0	48.2	374±56
SA02-610	0.13	39.78	1.93	42.56	0.01	0.02	1.85	0.026	0.108	8.24	4.40	99.1	<0.5	<0.1	<0.1	<0.1	0	64.9	259±14
SA02-611	0.20	38.91	2.17	42.86	<0.01	0.03	1.95	0.020	0.111	7.95	4.55	98.8	3.3	<0.1	<0.1	<0.1	0	84.7	269±27
SA02-612	0.49	39.01	1.74	43.43	<0.01	<0.01	1.61	0.023	0.104	8.70	3.69	98.8	1.4	<0.1	<0.1	<0.1	0	220.0	180±29
SA05-618	0.05	43.12	1.88	43.67	<0.01	0.06	1.41	0.029	0.121	8.69	<0.01	99.0	5.9	<0.1	<0.1	0.7	<0.1	87.3	231±10
SA05-618-A	0.05	43.12	1.88	43.67	<0.01	0.06	1.41	0.029	0.121	8.69	<0.01	99.0	5.9	<0.1	<0.1	0.7	<0.1	74.7	274±11
SA05-619	0.05	41.12	1.61	41.98	<0.01	0.03	1.60	0.022	0.115	8.36	5.03	99.9	7.3	<0.1	<0.1	<0.1	<0.1	90.9	408±15
Northwest Valley																			
SA05-616	0.02	42.46	0.94	41.40	<0.01	0.04	0.71	0.006	0.102	7.88	6.26	99.8	7.9	<0.1	<0.1	0.1	<0.1	89.1	141±12
SA05-616-A	0.02	42.46	0.94	41.40	<0.01	0.04	0.71	0.006	0.102	7.88	6.26	99.8	7.9	<0.1	<0.1	0.1	<0.1	92.1	167±5
SA05-613	0.04	43.62	0.96	43.08	<0.01	<0.01	0.93	0.012	0.114	8.32	2.96	100.0	10.5	<0.1	<0.1	<0.1	<0.1	77.3	48±3
SA05-617	0.06	40.88	1.94	41.93	<0.01	<0.01	1.93	0.033	0.114	8.31	4.68	99.9	5.6	<0.1	<0.1	<0.1	<0.1	102.3	197±9
SA05-617-A	0.06	40.88	1.94	41.93	<0.01	<0.01	1.93	0.033	0.114	8.31	4.68	99.9	5.6	<0.1	<0.1	<0.1	<0.1	117.8	186±8

[a]Loss on ignition.

inferred central ice flow line of the Kartal Lake glacier (Fig. 2). Our model uses the flow line starting at the elevation of 2230 m on the rim of the plateau and continues down to 1778 m, which is 122 m below the lowest moraine in the Kartal Lake Valley. The total length of the flow line in the model is 2 km, well in excess of the distance to the outermost moraines, which are situated 1.5 km away from the plateau rim.

Long term monthly mean temperature and precipitation data from the Global Historical Climatology Network (version 2, http://www.ncdc.noaa.gov/oa/climate/ghcn-monthly/index.php, accessed in May 2007) was used. Because of the sharp gradient of continentality over the region (Kurupınar, 1995; Kadıoğlu, 2000; Ünal et al., 2003), we used only those weather stations that are within 200 km radius of Mount Sandıras to project monthly temperature and precipitation on the mountain. We restricted to use of weather station data that have at least 30 years of coverage. First, for each month, weather station temperature was transferred to sea level using the modern air temperature lapse rate calculated from the radiosonde data (http://raob.fsl.noaa.gov/, accessed in May 2007) at Isparta station (165 km northeast of Sandıras, Fig. 1). Then, the data were kriged using the ArcGIS software (version 9.1). The surface temperatures along the Kartal Lake Valley were then recalculated using the same lapse rates for each month from the interpolated values. Precipitation rates on Mount Sandıras were calculated by interpolation of the same weather station data using the same kriging method over the region.

In the model, a 0 °C cutoff temperature is assumed to calculate the fraction of total precipitation in the valley that falls as snow. If the air temperature is below or equal to 0 °C, all precipitation is assumed to be snow, above that threshold—rain. The total annual accumulation of snow is determined using projected monthly precipitation rates and temperatures. Yearly ablation is calculated by determining the spatial distribution of positive degree days sums (Braithwaite, 1995) in the valley. Degree day factors of $3\,mm\,day^{-1}\,°C^{-1}$ (water equivalent) for snow and $8\,mm\,day^{-1}\,°C^{-1}$ for ice (Braithwaite and Zhang, 2000) are assumed, as is a standard deviation of 3.3 °C for the monthly mean surface temperature, which is based on the Isparta weather station data. Finally, glacier mass balance is calculated as snow accumulation minus ablation and the ELA is defined as the elevation at which the computed mass balance is zero.

We have tested the model results by calculating the paleo-ELA of LGM glaciers using different methods. Our model yielded a zero mass balance at 1998 m for the conditions which Kartal Lake moraines deposited. The accumulation area ratio (AAR) method (Porter, 1975), with the AAR value of 0.6 (Nesje and Dahl, 2000) and the reconstructed area of an LGM glacier of 0.77 km^2, gave a comparable value of 1975 m. Both figures are consistent with the calculations made by de Planhol (1953) and Doğu (1993).

5. Results

5.1. Cosmogenic ^{36}Cl exposure ages

We dated six boulders from the Kartal Lake Valley and three from the Northwest Valley (Fig. 2; Table 1). All boulder ages include correction for thickness and shielding by surrounding topography and snow. The uncertainties quoted for the boulder ages were calculated by propagation of analytical errors on $^{36}Cl/Cl$ and on Cl (both reported by the AMS laboratory) and assuming a 20% uncertainty on the calculated nucleogenic component. Boulder age uncertainties are based only on analytical errors and given at the $1\sigma_d$ (standard deviation) level. Moraine ages are calculated as weighted mean of boulder ages, and are given at the $1\sigma_{em}$ (standard error of the mean) level. Total errors, reported in Table 1, include both analytical errors and uncertainties on production rates of ^{36}Cl.

With the exception of one older outlier, the boulders from Kartal Lake moraines have ages ranging from 17.2 ± 2.9 ka to 22.1 ± 3.3 ka (Table 1). Samples SA02-609, 610 and 611 are from moraine A1, and have a weighted mean age of 20.4 ± 1.3 ka. Samples SA02-612, SA05-618, 618-A and 619 are from moraine A2 in the same valley. Sample 619 gave an age of 34.7 ± 1.3 ka. Because it is older than all other samples by more than six standard deviations, we consider it an older outlier, probably containing ^{36}Cl inherited from episodes of previous exposure to cosmic radiation. This sample was excluded from further consideration. Samples 618-A is the open vessel replicate of sample 618. For further calculations, replicates are internally weighted averaged first and this average added to the moraine age calculations. Therefore, samples 612 and 618 gave ages of 17.2 ± 2.9 ka and 20.6 ± 1.3 ka, and the age of moraine A2 is calculated as 19.6 ± 1.6 ka. Although ages of moraine A1 and A2 overlap at the 1-sigma level, the stratigraphic positions of these moraines suggest that the former indicates the maximum position of the glaciers, and the latter records a readvance.

Samples SA05-616 and its replicate 616-A, from the outer ridge of terminal moraine B1 in the Northwest Valley, yielded ages of 14.8 ± 1.2 ka and 17.2 ± 0.6 ka, respectively, and sample SA05-617 and 617-A, from the outer ridge of terminal moraine B2, yielded ages of 16.4 ± 0.8 ka and 16.0 ± 0.7 ka (Table 1). Thus, B1 and B2 moraine ages are 16.5 ± 1.1 ka and 16.2 ± 0.5 ka, respectively. Sample SA05-613, from the innermost moraine gave a young age of 5.1 ± 0.3 ka. This boulder is small (70×50 cm) and short (height of 40 cm), and its young age could be due to post-depositional modification that affected its exposure to cosmic radiation. However, given the position of the sample on the innermost moraine crest (Fig. 2), it is also possible that the age is real, and that there was a glacial advance in the Middle Holocene. Additional samples are needed to test this hypothesis. For the purposes of this paper, which concentrates on the LGM, this sample is excluded from further consideration.

The cosmogenic ^{36}Cl ages suggest that the glaciers started retreating from their maximum positions by 20.4 ± 1.3 ka ago. Two later readvances ended 19.6 ± 1.6 ka ago in the Kartal Lake Valley and 16.2 ± 0.5 ka ago in the Northwest Valley. These results agree with other glacial records in the Mediterranean area (Hughes et al., 2006a), and particularly with the recent glacial geological studies in Turkey (Akçar et al., 2007; Zahno et al., 2007) that showed LGM ages of recent glacial deposits. The advance of glaciers in the Kaçkar Mountains, near the Black Sea, began at least 26.0 ± 1.2 ka ago and continued until 18.3 ± 0.9 ka (Akçar et al., 2007). Similar results were reported from Dedegöl Mountains, southwest Turkey by Zahno et al. (2007) who measured cosmogenic ^{10}Be ages of moraines and claimed that LGM glaciation started 26 ka ago and continued until 19 ka ago. Thus, all three cosmogenic records indicate maximum glacial activity during the LGM and deglaciation shortly thereafter.

5.2. Paleoclimatic interpretation

Modeled glacier lengths as a function of temperature and precipitation changes from modern conditions are plotted in Fig. 4. The contours show how the length of glacier in the Kartal Lake Valley varies with climate. The zero

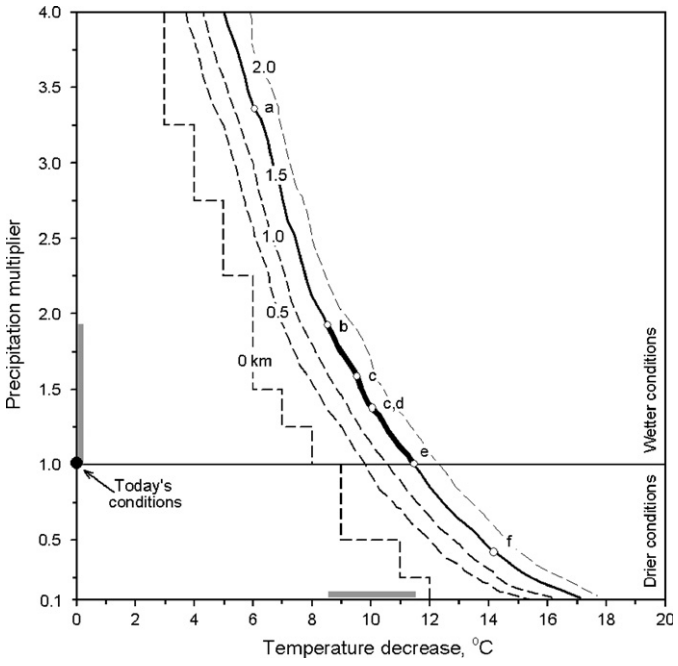

Fig. 4. Modeled length of the Kartal Lake Valley glacier (solid line) as a function of temperature and precipitation changes from those of today (full circle). As a comparison 0 km line which represents glacier inception and 0.5, 1 and 2 km lines shown (dashed lines). Thick solid and corresponding horizontal and vertical gray lines are suggested possible ranges of temperature and precipitation changes during LGM. Empty circles are those conditions suggested by proxy data (a: Bar-Matthews et al., 1997, b: Hughes et al., 2003, c: Emeis et al., 1998, 2000; Kallel et al., 2000, d: McGarry et al., 2004, e: corresponds to threshold temperature depression to sustain glacier by same amount of moisture level as today (proposed by this study), f: Jones et al., 2007).

kilometer line represents the threshold values for glaciation; no glaciers can exist to the left and below this line. The model results show that under the modern temperature and precipitation conditions glaciers will not form on the mountain, which is consistent with field observations. Possible combinations of climatic conditions that produced the Kartal Lake Valley glacier are along the line labeled 1.5 km. They encompass wide ranges of temperature and precipitation, including those that are highly unlikely (e.g., extremely high precipitation rates would have to accompany moderate decreases of temperature). Glacier modeling shows that a cooling of about 11.5 °C is needed if we assume the same precipitation rate as today, less than 11.5 °C of cooling would require greater precipitation than modern (wetter conditions), and greater temperature depressions would require less than modern precipitation (drier conditions) to sustain glaciers on Mount Sandıras. In order to reduce these possible ranges, we employed additional information from other paleoclimate proxy data around the region, especially paleotemperature estimates since they are easier than the prediction of paleoprecipitation.

Bar-Matthews et al. (1997) reconstructed the eastern Mediterranean paleoclimate during the past 25 ka using a high resolution petrographic, stable isotopic, and age study of speleothems from the Soreq Cave, Israel (Fig. 1 for location). They showed that during the period from 25 ka ago to 17 ka ago the eastern coast of the Levantine Basin was characterized by air temperatures about 6 °C lower than today and annual precipitation was 20–50% lower than today. Mean annual temperatures in Jerusalem and in Köyceğiz (15 km southwest of Mount Sandıras) are 17.0 and 18.3 °C, respectively. Although the precipitation rates of the two regions are different (the Israeli coast is drier than the southwest coast of Turkey), their seasonal variations are similar (Stevens et al., 2001). In Jerusalem, 67% of precipitation falls in the winter, from December to February, and in Köyceğiz the corresponding value is 57%. Furthermore, precipitation sources for these two regions are the Mediterranean Sea (Kendrew, 1961; Wigley and Farmer, 1982; Stevens et al., 2001). Vaks et al. (2006) studied $\delta^{18}O$ in speleothems from four caves of the Northern Negev Desert and found that during the last 200 ka the source of rainfall in northern Negev area was the Eastern Mediterranean. Because today the area of the Soreq Cave has similar climate to that of the southwestern Turkey, it is likely that this temperature shift is representative of the wider region, and can be applied to constrain the LGM temperature at Sandıras. For the first approximation, we assume that during the period from 25 ka ago to 17 ka ago, the temperature at Mount Sandıras was lower by the same amount as that in the Soreq Cave. Moreover, because the Soreq Cave is 400 m above sea level while Sandıras is well above this elevation, it is likely that the 6 °C cooling inferred for the Soreq Cave is a minimum cooling expected at Mount Sandıras. To produce glaciers on Mount Sandıras, this moderate cooling would have to be accompanied by precipitation ~3.3 times higher than today, which is unlikely. If the prescribed precipitation level from Soreq Cave is used, this will make the LGM temperatures on Mount Sandıras 12–13.5 °C colder than today (Fig. 4).

In order to obtain better estimates of terrestrial temperatures in the Eastern Mediterranean, McGarry et al. (2004) measured the hydrogen-isotopic composition (δD) of speleothems fluid inclusions from three caves including the Soreq Cave in Israel and showed that the LGM temperature was about 10 °C cooler than today. A similar amount of cooling, 9.5–10 °C, was obtained from the alkenone and $\delta^{18}O$ records in sediment cores from the Mediterranean Sea (Emeis et al., 2000), in Levantine basin (Kallel et al., 2000) and Crete (Emeis et al., 1998). Furthermore, these data are in good agreement with land-based reconstructions of temperatures and precipitation rates (Bar-Matthews et al., 2003). Assuming a 10 °C cooling during the LGM, our model results indicate a precipitation rate that is 1.3 times higher than the modern value (Fig. 4). Both results from the Soreq Cave and deep sea cores in the Mediterranean Sea, when fed into our glacial model, imply a wet and cold LGM on Mount Sandıras.

Humid and cold climate during LGM on Mount Sandıras is also supported by reconstruction of paleoclimate in Greece. Hughes et al. (2003, 2006b) used the geological record of glaciers and rock glaciers on Pindus Mountains and suggested that the Würm glacier stage was 8.5 °C (8–9 °C) cooler and slightly wetter (~1.1 times) than today. If we assume the same amount of cooling on Mount Sandıras, the LGM precipitation would have to almost double (1.9 times more than modern). If we assume their paleoprecipitation estimates, our model yields 11 °C of cooling.

Further north, in Anatolia, although there is generally agreement on colder condition during the LGM, contemporary moisture levels are incongruous. Lacustrine facies analyses on Konya plain show that lake levels were high at and prior to the LGM (Roberts, 1983; Kuzucuoğlu et al., 1999; Roberts et al., 1999, 2001) and the data is consistent with other lakes in Turkey (Roberts and Wright, 1993; Kashima, 2002). High lake stands are indicative of high input of water (wetter conditions) or lower evaporation to precipitation rates which indicate lower temperatures. Jones et al. (2007) studied Eski Acıgöl, a closed basin lake in Central Anatolia, using hydrological and isotope mass balance models and reported that glacial time (between 23 and 16 ka before present) precipitation was 63% drier than today, in agreement with palynological studies. Van Zeist et al. (1975) show steppe and almost treeless vegetation implying that the climate was dry in southwestern Turkey during LGM. In contrast, marine pollen records from the Marmara Sea (Mudie et al., 2002) revealed LGM climate slightly wetter on the mountains that surround the Marmara Sea. For drier LGM, if we assume that the precipitation was 60% less, our modeling

results reveal that accompanying temperatures should be depressed by about 14 °C (Fig. 4).

In conclusion, there is no consensus regarding the moisture levels in the region during the LGM. While some researchers suggest that it was drier (van Zeist et al., 1975; Robinson et al., 2006; Jones et al., 2007) others think the opposite (Gvirtzman and Wieder, 2001; Mudie et al., 2002; Hughes et al., 2003). Furthermore, paleoprecipitation values change from region to region, coastal areas versus interiors (Jones et al., 2007), which imply that local climate factors played an important role. Because of these uncertainties, we prefer to use a range of paleotemperature estimates and report the paleoprecipitation conditions rather than report a fixed value for either one. If the extreme case of cooling by only 6 °C (Bar-Matthews et al., 1997) is ignored, as highly unlikely, other temperature estimates are in the range of between 10 and 8.5 °C. Our analysis of paleoconditions on Mount Sandıras suggests that the use of the Hughes et al.'s (2003) estimate of 8.5 °C as a minimum limit of cooling on Mount Sandıras will almost double the precipitation rates necessary to produce glaciers consistent with the observed moraines on Kartal Lake Valley (Fig. 4). Up to 11.5 °C of cooling sustain wetter conditions.

Our present day climate estimates on Mount Sandıras, at an elevation of 2000 m, which is close to the LGM time ELA, is calculated as annual average temperature of about 6 °C and annual precipitation of about 1 m. Our model results show that under the wetter conditions (1–1.9 m), the cooling by 8.5–11.5 °C will bring the mean annual temperature to between −5.5 and −2.5 °C at 2000 m on Mount Sandıras.

6. Conclusion

The most extensive glacial advance on Mount Sandıras ended by 20.4 ± 1.3 ka ago, and the final deglaciation commenced by 16.2 ± 0.5 ka ago. Modeling of glacier mass balance shows a wide range of possible temperatures and precipitation rates necessary to produce Mount Sandıras glaciers. Without independent estimates of temperature and precipitation for LGM, model results do not provide a unique combination of these variables based on simulated ice extent. An LGM half as wet as today requires a cooling by 13.5 °C, whereas an LGM twice as wet as today requires a cooling by 8.5 °C. By employing published paleoclimate proxy data, the range can be reduced significantly. However, the temperature estimates from the proxy data indicate no more than 10 °C of cooling during the LGM in the Eastern Mediterranean. Assuming this published temperature range, the model yields up to 1.9 times higher precipitation rate which indicates wetter conditions during the LGM on the study area. This is supported by high lake levels in and around Anatolia, but not by palynological analysis which is sensitive to unique set of variables, including seasonality changes. Our results imply high moisture levels during LGM for the southwest coasts of Anatolia. This is at odds with the conventional view of LGM being cold and dry in Anatolia and the Eastern Mediterranean.

Acknowledgments

This research was supported by the US National Science Foundation (Grant 0115298) and by the Scientific and Technological Research Council of Turkey (TÜBİTAK) (Grant 101Y002).

References

Akçar, N., Yavuz, V., Ivy-Ochs, S., Kubik, P.W., Vardar, M., Schluchter, C., 2007. Paleoglacial records from Kavron Valley, NE Turkey: field and cosmogenic exposure dating evidence. Quaternary International 164–165, 170–183.

Almasi, P.F., 2001. Dating the paleobeaches of Pampa Mejillones, Northern Chile by cosmogenic chlorine-36. M.S. Thesis, University of Arizona, Tucson AZ, USA.

Anderson, K.M., Bradley, E., Zreda, M., Rassbach, L., Zweck, C., Sheehan, E., 2007. ACE: Age Calculation Engine—a design environment for cosmogenic dating techniques. In: Proceedings of the International Conference on Advanced Engineering Computing and applications in Sciences, Papeete, Tahiti, pp. 39–48.

Aruscavage, P.J., Campbell, E.Y., 1983. An ion-selective electrode method for determination of chlorine in geological materials. Talanta 30, 745–749.

Atalay, I., 1987. Introduction to Geomorphology of Turkey, second ed. Ege University Press, İzmir, Turkey (in Turkish).

Bar-Matthews, M., Ayalon, A., Kaufman, A., 1997. Late Quaternary paleoclimate in the Eastern Mediterranean region from stable isotope analysis of speleothems at Soreq Cave, Israel. Quaternary Research 47, 155–168.

Bar-Matthews, M., Ayalon, A., Gilmour, M., Matthews, A., Hawkesworth, C., 2003. Sea-land oxygen isotopic relationships from planktonic foraminifera and speleothems in the Eastern Mediterranean region and their implications for paleorainfall during interglacial intervals. Geochimica et Cosmochimica Acta 67, 3181–3199.

Birman, J.H., 1968. Glacial reconnaissance in Turkey. Geological Society of America Bulletin 79, 1009–1026.

Braithwaite, R.J., 1995. Positive degree-day factors for ablation on the Greenland ice sheet studied by energy-balance. Journal of Glaciology 41, 153–160.

Braithwaite, R.J., Zhang, Y., 2000. Sensitivity of mass balance of five Swiss glaciers to temperature changes assessed by tuning a degree-day model. Journal of Glaciology 46 (152), 7–14.

Çiner, A., 2004. Turkish glaciers and glacial deposits. In: Ehlers, J., Gibbard, P.L. (Eds.), Quaternary Glaciations: Extent and Chronology, Part I: Europe. Elsevier Publishers, Amsterdam, pp. 419–429.

Collins, A.S., 1997. Tectonic evolution of Tethys in the Lycian Taurides, southwest Anatolia. Ph.D. Thesis, University of Edinburgh, Edinburgh, Scotland.

Collins, A.S., Robertson, A.H.F., 1998. Processes of Late Cretaceous to Late Miocene episodic thrust-sheet translation in the Lycian Taurides, SW Turkey. Journal of the Geological Society, London 155, 759–772.

Davis, R.J., Schaeffer, O.A., 1955. Chlorine-36 in nature. Annals of the New York Academy of Science 62, 105–122.

de Graciansky, P.C., 1967. Existance d'une nappe ophiolitique à l'extrémité occidentale de la chaîne sud-anatolienne; relations avec les autres unités charriées avec terrains autochtones (Province de Muğla, Turquie). Comptes Rendus de l'Academie des Sciences, Paris 264, pp. 2876–2879.

de Planhol, X., 1953. Les formes glaciaires du Sandıras Dag et la limite des neiges eternelles quaternaries dans le SW de l'Anatolie. Compte Rendu Sommaire de la Societe Geologique de France, pp. 263–265.

Desilets, D., Zreda, M., 2003. Spatial and temporal distribution of secondary cosmic-ray nucleon intensities and applications to in situ cosmogenic dating. Earth and Planetary Science Letters 206, 21–42.

Desilets, D., Zreda, M., Probe, T., 2006a. Extended scaling factors for in situ cosmogenic nuclides: new measurements at low latitude. Earth and Planetary Science Letters 246, 265–276.

Desilets, D., Zreda, M., Almasi, P.F., Elmore, D., 2006b. Determination of cosmogenic ^{36}Cl in rocks by isotope dilution: innovations, validation and error propagation. Chemical Geology 233 (3–4), 185–195.

Doğu, A.F., 1986. Geomorphology of Koycegiz and Dalaman lowland and surrounding area (in Turkish). Ph.D. Thesis, Ankara University, Ankara, Turkey.

Doğu, A.F., 1993. Glacier shapes on the Mount Sandıras. Turkish Geography Bulletin, Ankara University 2, 263–274 (in Turkish).

Doğu, A.F., 1994. The importance of Akkopru terraces (Dalaman River) in geomorphology of southwest Anatolia. Turkish Geography Bulletin, Ankara University 3 (in Turkish).

Ehlers, J., 1996. Quaternary and Glacial Geology. Wiley, Chichester.

Elsheimer, H.N., 1987. Application of an ion-selective electrode method to the determination of chloride in 41 international geochemical reference materials. Geostandards Newsletter 11, 115–122.

Emeis, K.C., Schulz, H.M., Struck, U., Sakamoto, T., Doose, H., Erlenkeuser, H., Howell, M., Kroon, D., Paterne, M., 1998. Stable isotope and alkenone temperature records of sapropels from sites 964 and 967: constraining the physical environment of sapropel formation in the Eastern Mediterranean Sea. In: Robertson, et al. (Eds.), Proceedings of the Ocean Drilling Program, vol. 160, pp. 309–331.

Emeis, K.C., Struck, U., Schulz, H.M., Rosenberg, R., Bernasconi, S., Erlenkeuser, H., Sakamoto, T., Martinez-Ruiz, F., 2000. Temperature and salinity variations of Mediterranean Sea surface waters over the last 16 000 years from records of planktonic stable oxygen isotopes and alkenone unsaturation ratios. Palaeogeography Palaeoclimatology Palaeoecology 158, 259–280.

Engin, T., Hirst, D.M., 1970. The Alpine chrome ores of the Andızlık-Zımparalık area, Fethiye, SW Turkey. Mineralogical Magazine 38, 76–82.

Erinç, S., 1952. Glacial evidences of the climatic variations in Turkey. Geografiska Annaler 34, 89–98.

Erinç, S., 1971. Geomorphology, second ed. Istanbul University Geography Institute Press, Istanbul (in Turkish).

Erinç, S., 1978. Changes in the physical environment in Turkey since the end of last glacial. In: Brice, W.C. (Ed.), The Environmental History of the Near and Middle East Since the Last Ice Age. Academic Press, London, pp. 87–110.

Fairbanks, R.G., 1989. A 17 000-year glacio-eustatic sea level record: influence of glacial melting rates on the Younger Dryas event and deep-ocean circulation. Nature 342, 637–642.

Gosse, J.C., Phillips, F.M., 2001. Terrestrial in-situ cosmogenic nuclides: theory and application. Quaternary Science Reviews 20, 1475–1560.

Guyodo, Y., Valet, J.P., 1999. Global changes in intensity of the Earth's magnetic field during the past 800 ka. Nature 399, 249–252.

Gvirtzman, G., Wieder, M., 2001. Climate of the last 53,000 years in the Eastern Mediterranean based on soil-sequence stratigraphy in the coastal plain of Israel. Quaternary Science Reviews 20, 1827–1849.

Haeberli, W., 1996. Glacier fluctuations and climate change detection. Geografia Fisica e Dinamica Quarternaria 18, 191–199.

Hughes, P.D., Gibbard, P.L., Woodward, J.C., 2003. Relict rock glaciers as indicators of Mediterranean palaeoclimate during the Last Glacial Maximum (Late Würmian) in northwest Greece. Journal of Quaternary Science 18 (5), 431–440.

Hughes, P.D., Woodward, J.C., Gibbard, P.L., 2006a. Quaternary glacial history of the mediterranean mountains. Progress in Physical Geography 30 (3), 334–364.

Hughes, P.D., Woodward, J.C., Gibbard, P.L., 2006b. Late Pleistocene glaciers and climate in the Mediterranean. Global and Planetary Change 50 (1–2), 83–98.

Jones, M.D., Roberts, N.C., Leng, M.J., 2007. Quantifiying climatic change through the last glacial-interglacial transition based on lake isotope paleohydrology from central Turkey. Quaternary Research 67, 463–473.

Kaaden, G., 1959. On the relationship between the composition of chromites and their tectonic-magmatic position in peridotite bodies in the SW of Turkey. Bulletin Maden ve Tetkik Arama Enstitüsü (Ankara) 52, 1–14.

Kadıoğlu, M., 2000. Regional variability of seasonal precipitation over Turkey. International Journal of Climatology 20 (14), 1743–1760.

Kallel, N., Duplessy, J.C., Labeyrie, L., Fontugne, M., Paterne, M., Montacer, M., 2000. Mediterranean and pluvial periods and sapropel formation during last 200 000 years. Palaeogeography Palaeoclimatology Palaeoecology 157, 45–58.

Kashima, K., 2002. Environmental and climatic changes during the last 20 000 years at Lake Tuz, Central Turkey. Catena 48, 3–20.

Kendrew, W.G., 1961. The Climates of the Continents, fifth ed. Oxford Press, London.

Klimchouk, A., Bayarı, S., Nazik, L., Törk, K., 2006. Glacial destruction of cave systems in high mountains, with a special reference to the Aladaglar Massif, Central Taurus, Turkey. Acta Carsologica 35 (2), 111–121.

Kurter, A., 1991. Glaciers of Middle East and Africa—glaciers of Turkey. In: Williams, R.S., Ferrigno, J.G., (Eds.), Satellite Image Atlas of the World. USGS Professional Paper 1386-G-1, pp. 1–30.

Kurter, A., Sungur, K., 1980. Present glaciation in Turkey. In: World Glacier Inventory, International Association of Hydrological Sciences 126, Switzerland, pp. 155–160.

Kurupınar, M., 1995. Investigation of the topographical effects on the precipitation distribution over Turkey by satellite data. International Geoscience and Remote Sensing Symposium, Firenze, Italy, pp. 371–373.

Kuzucuoğlu, C., Bertaux, J., Black, S., Denefle, M., Fontugne, M., Karabıyıkoğlu, M., Kashima, K., Limondin-Lozouet, N., Mouralis, D., Orth, P., 1999. Reconstruction of climatic changes during the Late Pleistocene based on sediment records from the Konya Basin (Central Anatolia, Turkey). Geological Journal 34 (1–2), 175–198.

la Fontaine, C.V., Bryson, R.A., Wendland, W.M., 1990. Airstream regions of North Africa and the Mediterranean. Journal of Climate 3, 366–372.

Mackintosh, A.N., Barrows, T.T., Colhoun, E.A., Fifield, L.K., 2006. Exposure dating and glacial reconstruction at Mount Field, Tasmania, Australia, identifies MIS 3 and MIS 2 glacial advances and climatic variability. Journal of Quaternary Science 21 (4), 363–376.

Macklin, M.G., Fuller, I.C., Lewin, J., Maas, G.S., Passmore, D.G., Rose, J., Woodward, J.C., Black, S., Hamlin, R.H.B., Rrowan, J.S., 2002. Correlation of fluvial sequences in the Mediterranean basin over the last 200 ka and their relationship to climate change. Quaternary Science Reviews 21 (14–15), 1633–1641.

McGarry, S., Bar-Matthews, M., Matthews, A., Vaks, A., Schilman, B., Ayalon, A., 2004. Constraints on hydrological and paleotemperature variations in the Eastern Mediterranean region in the last 140 ka given by the δD values of speleothem fluid inclusions. Quaternary Science Reviews 23, 919–934.

Messerli, B., 1967. Die eiszeitliche und die gegenwartige Vergletscherung in Mittelmeerraum. Geographica Helvetica 22, 105–228.

Mudie, P.J., Rochon, A., Aksu, A.E., 2002. Pollen stratigraphy of Late Quaternary cores from Marmara Sea: land-sea correlation and paleoclimatic history. Marine Geology 190, 233–260.

Nesje, A., Dahl, S.O., 2000. Glaciers and Environmental Change: Key Issues in Environmental Change Series. Oxford University Press, London.

Ohno, M., Hamano, Y., 1992. Geomagnetic poles over the last 10 000 years. Geophysical Research Letters 19 (16), 1715–1718.

Onde, H., 1952. Formes glaciaires dans le massif Lycien de l'Ak dag (Turquie du S.-O.). XIX Congres geologique International, pp. 327–335.

Owen, L.A., Gualtieri, L., Finkel, R.C., Caffee, M.W., Benn, D.I., Sharma, M.C., 2001. Cosmogenic radionuclide dating of glacial landforms in the Lahul Himalaya, northern India: defining the timing of Late Quaternary glaciation. Journal of Quaternary Science 16 (6), 555–563.

Owen, L.A., Finkel, R.C., Caffee, M.W., Gualtieri, L., 2002. Timing of multiple late Quaternary glaciations in the Hunza Valley, Karakoram Mountains, northern Pakistan: defined by cosmogenic radionuclide dating of moraines. GSA Bulletin 114, 593–604.

Paterson, W.S.B., 1994. The Physics of Glaciers, third ed. Pergamon, Oxford.

Philippson, A., 1915. Reisen und Forschungen im westlichen Kleinasien, Gotha, Petermanns Geigr. Mitteilungen Heft 1–5, 167–183.

Phillips, F.M., Leavy, B.D., Jannik, N.O., Elmore, D., Kubik, P.W., 1986. The accumulation of cosmogenic Chlorine-36 in rocks: a method for surface exposure dating. Science 231, 41–43.

Phillips, F.M., Zreda, M.G., Flinsch, M.R., Elmore, D., Sharma, P., 1996. A reevaluation of cosmogenic ^{36}Cl production rates in terrestrial rocks. Geophysical Research Letters 23 (9), 949–952.

Phillips, F.M., Stone, W.D., Fabryka-Martin, J., 2001. An improved approach to calculating low-energy cosmic ray neutron fluxes near the land/atmosphere interface. Chemical Geology 175, 689–701.

Pons, L.J., Edelman, C.H., 1963. Soil investigations in Koycegiz and Dalaman (in Turkish). Toprak ve gübre araştırmaları Enst. Müd., Toprak etüdleri serisi 5, Ankara.

Porter, S.C., 1975. Equilibrium-line altitudes of late Quaternary glaciers in the Southern Alps, New Zealand. Quaternary Research 5, 27–47.

Principato, S.M., Geirsdóttir, Á., Jóhannsdóttir, G.E., Andrews, J.T., 2006. Late Quaternary glacial and deglacial history of eastern Vestfirdir, Iceland using cosmogenic isotope (^{36}Cl) exposure ages and marine cores. Journal of Quaternary Science 21, 271–285.

Roberts, N., 1983. Age, paleoenvironments and climatic significance of Late Pleistocene Konya Lake, Turkey. Quaternary Research 19, 154–171.

Roberts, N., Wright Jr., H.E., 1993. Vegetational, lake-level and climatic history of the Near East and Southwest Asia. In: Wright, Jr., H.E., Kutzbach, J.E., Webb, III, T., Ruddiman, W.F., Street-Perrott, F.A., Bartlein, P.J. (Eds.), Global Climates Since the Last Glacial Maximum. University of Minnesota Press, Minneapolis, pp. 194–220.

Roberts, N., Black, S., Boyer, P., Eastwood, W.J., Leng, M., Parish, R., Reed, J., Twigg, D., Yiğitbaşıoğlu, H., 1999. Chronology and stratigraphy of Late Quaternary sediments in the Konya Basin, Turkey: results from the KOPAL Project. Quaternary Science Reviews 18, 611–630.

Roberts, N., Reed, J.M., Leng, M.J., Kuzucuoğlu, C., Fontugne, M., Bertaux, J., Woldring, H., Bottema, S., Black, S., Hunt, E., Karabıyıkoğlu, M., 2001. The tempo of Holocene climatic change in the eastern Mediterranean region: new high-resolution crater-lake sediment data from central Turkey. Holocene 11 (6), 721–736.

Robinson, S.A., Black, S., Sellwood, B.W., Valdes, P.J., 2006. A review of paleoclimates and paleoenvirments in the Levant and Eastern Mediterranean from 25 000 to 5 000 years BP: setting the environmental background for the evolution of human civilization. Quaternary Science Reviews 25, 1517–1541.

Stevens, L.R., Wright Jr., H.E., Ito, E., 2001. Proposed changes in seasonality of climate during the Lateglacial and Holocene at Lake Zeribar, Iran. Holocene 11 (6), 747–755.

Stone, J.O.H., Evans, J.M., Fifield, L.K., Cresswell, R.G., Allan, G.L., 1996. Cosmogenic chlorine-36 production rates from calcium and potassium. Radiocarbon 38 (1), 170–171.

Stone, J.O.H., Evans, J.M., Fifield, L.K., Allan, G.L., Cresswell, R.G., 1998. Cosmogenic chlorine-36 production in calcite by muons. Geochimica et Cosmochimica Acta 62 (3), 433–454.

Swanson, T.W., Caffee, M.L., 2001. Determination of ^{36}Cl production rates derived from well dated deglaciation surfaces of Whidbey and Fidalgo Islands, Washington. Quaternary Research 56, 366–382.

Ünal, Y., Kindap, T., Karaca, M., 2003. Redefining the climate zones of Turkey using cluster analysis. International Journal of Climatology 23 (9), 1045–1055.

Vaks, A., Matthews, M.B., Ayalon, A., Matthews, A., Frumkin, A., Dayan, U., Halicz, L., Almogi-Labin, A., Schilman, B., 2006. Paleoclimate and location of the border between Mediterranean climate region and the Saharo-Arabian Desert as revealed by speleothems from the northern Negev Desert, Israel. Earth and Planetary Science Letters 249 (3–4), 384–399.

van Zeist, W., Woldring, H., Stapert, D., 1975. Late Quaternary vegetation and climate of south western Turkey. Palaeohistoria 7, 53–143.

Wigley, T.M.L., Farmer, G., 1982. Climate of the Eastern Mediterranean and Near East. In: Bintliff, J.L., Van Zeist, W. (Eds.), Paleoclimates, Paleoenvironments and Human Communities in the Eastern Mediterranean Region in Later Prehistory. B.A.R. International Series 133 (1), pp. 3–37.

Yang, S., Odah, H., Shaw, J., 2000. Variations in the geomagnetic dipole moment over the last 12 000 years. Geophysical Journal International 140, 158–162.

Zahno, C., Akçar, N., Yavuz, V., Kubik, P., Schluchter, C., 2007. Determination of cosmogenic surface ages of paleoglaciers of southwest Anatolia and paleoclimatic interpretations. In: VI. Quaternary Workshop of Turkey. Istanbul Technical University, Istanbul, Turkey (in Turkish).

Zreda, M.G., Phillips, F.M., 2000. Cosmogenic nuclide buildup in surficial materials. In: Noller, J.S., Sowers, J.M., Lettis, W.R. (Eds.), Quaternary Geochronology: Methods and Applications, AGU Reference Shelf 4, American Geophysical Union, pp. 61–76.

Zreda, M.G., Phillips, F.M., Elmore, D., Kubik, P.W., Sharma, P., 1991. Cosmogenic Chlorine-36 production rates in terrestrial rocks. Earth and Planetary Science Letters 105, 94–109.

Zreda, M., England, J., Phillips, F., Elmore, D., Sharma, P., 1999. Unblocking of the Nares Strait by Greenland and Ellesmere ice-sheet retreat 10 000 years ago. Nature 398, 139–142.

Zreda, M., Zweck, C., Sarıkaya, M.A., 2006. Early Holocene Glaciation in Turkey: Large Magnitude, Fast Deglaciation and Possible NAO Connection. American Geophysical Union Conference, San Fransisco, USA PP43A-1232.

Zweck, C., Zreda, M., Anderson, K., Bradley, L., 2006. iCronus: a computational tool for cosmogenic nuclide dating. American Geophysical Union Conference, San Francisco, USA, T11A-0425.